Simulation of second-order velocity slip of magnetohydrodynamic (MHD) flows

1st Thokozani Kunene
Mechanical and Industrial Engineering Technology Department, University of Johannesburg, Doornfontein Campus
Johannesburg, South Africa
tkunene@uj.ac.za

2nd Lagouge Tartibu
Mechanical and Industrial Engineering Technology Department, University of Johannesburg, Doornfontein Campus
Johannesburg, South Africa
ltartibue@uj.ac.za

***Abstract* — The influence of second-order velocity slip of magnetohydrodynamic flow involved in liquid-metal was numerically investigated. A commercial Computational Fluid Dynamics (CFD) code, STAR-CCM+ 13 was used. The MHD flow of Galinstan (GaInSn - Gallium-Indium-Tin) an electrically conducting liquid-metal fluid in the presence of a magnetic field was investigated. The variations of velocity within the second-order velocity slip parameters were found to be influenced by the local variations of the magnetic field. It was determined that the second-order velocity slip persists due to an increase in the thermal boundary layer. The numerical results were compared to published literature and were in good agreement.**

Keywords— Computational Fluid Dynamics, Liquid-metal, Magnetic field, Second-order velocity slip, Thermal boundary layer

I. INTRODUCTION

Magnetohydrodynamic (MHD) flows are fluids that electrically conductive in the presence of magnetic forces. The fluid flow of MHD as liquid metal is an interaction between the electromagnetic field and the fluid velocity field [1]. Slip flow is generally a nonphysical quantity termed as the slip length, which is a measure of the distance beyond the surface where velocity turns zero [2]. The slip of non-Newtonian fluids is best shown using the lattice Boltzmann (LB) simulations and Molecular Dynamics (MD) for the molecular-scale and intermolecular interactions [2]. Turkyilmazoglu showed that the shrinking sheet MHD slip flow of non-Newtonian fluid in the limit of no-slip coincides with the presence of a magnetic field that has considerable effects on velocity and temperature fields [3] [4].

The study of non-Newtonian Casson fluid under transverse magnetic field [5] has importance in many processes exist in different branches of science and technology. The investigation of the MHD flow of an electrically conducting fluid over a stretching surface is quite important in cooling systems of liquid metal [6].

The current study focuses on MHD fluids (electrically conducting fluid at room temperature) to investigate variations of velocity within the second-order velocity slip parameters. A numerical approach was taken to investigate the MHD flow in a mold design like the Faraday's open-cycle MHD generator with segmented electrodes [7] as shown in Figure 1.

II. NUMERICAL PROCEDURE

A. Geometry

The topology was created in Autodesk Inventor 2017 and imported to STAR-CCM+ 13 for Multiphysics module simulation of electromagnetism and hydrodynamic analysis. The magnetic arrangement and the electrodes are shown in Figure 1.

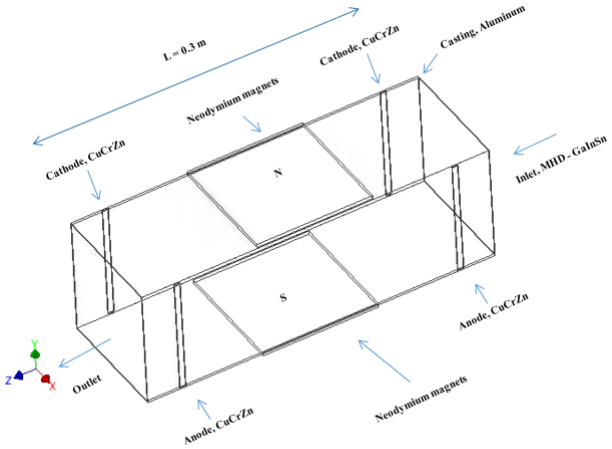

Figure 1. Faraday's open-cycle MHD generator with segmented electrodes [7].

B. Governing Equations

The governing equations of the steady flow of a liquid–metal as being articulated by Gedik *et al* [8], are present as:

Continuity equation

$$\nabla \cdot \mathbf{V} = 0 \qquad (1)$$

Conservation of momentum:

$$\rho(\partial V/\partial_t + (\mathbf{V}\cdot\nabla)\mathbf{V}) = -\nabla \mathbf{P} + \eta \nabla \cdot \mathbf{V} + [\mathbf{J}\times\mathbf{B}] \qquad (2)$$

Maxwell first law:

$$\nabla \times B = \mu e\, J \qquad \nabla \cdot B = 0 \qquad (3)$$

Ohm's law:

$$\mathbf{J} = \sigma[\mathbf{E}+\mathbf{V}\times\mathbf{B}] \qquad (4)$$

Where:

ρ is the density of the liquid-metal, V the velocity vector, η is the viscosity, the current density, B the total magnetic field of $\mathbf{B} = B_0+b$. B_0 and b are the applied external and induced magnetic field, respectively. **E** is the electrical field, $\boldsymbol{\mu_e}$ is the magnetic permeability and **σ** the electrical conductivity. The induced magnetic field is neglected due to the small magnetic Reynolds number approximation.

$$Ha = \mathbf{B}\, L\, (\boldsymbol{\sigma}/\boldsymbol{\mu_e})^{1/2} \qquad (5)$$

The dimensionless Hartmann number (Ha) is normally used to characterize the ratio of electromagnetic force to the viscous force in magnetohydrodynamic

Where:

L is the characteristic length of the MHD model.

Alam *et al* [9] presented the parameter of the slip as:

$$A = \frac{x^n a^{\frac{3(n-1)}{2}}}{v^{\frac{n-1}{2}}} \qquad (6)$$

Where *n* is a Casson parameter, a non-dimensional power-law is for fluid classification. A further deviation from unity indicates how far the fluid has deviated from being a Newtonian fluid. The Casson parameter would be:

$n < 1$ is pseudoplastic fluids; $n > 1$ for dilatant fluids and $n = 1$ is a Newtonian fluid. [9].

C. Mesh grid sensitivity study and Model validation

The grid sensitivity for the mesh structure, as noticed in Figure 2, elements of 204 748; 399 134; 454 078 and 488 367 were investigated for changes in the outlet pressure were of less than 8%. A grid of 368 185 elements was selected as suitable due to fewer fluctuation changes which account to a stable and accurate model. It further assists with the conservation of computing power.

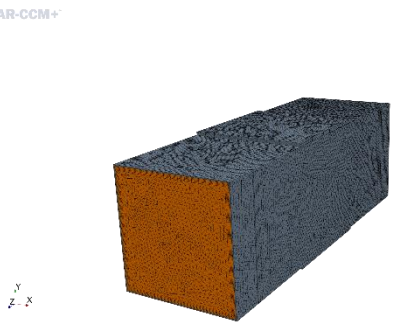

Figure 2. Mesh generated tetrahedral elements of 454 078 cells

The model was validated from a single magnate arrangement as seen from Figure 3 and Figure 4 shows an external application of magnetic fields of 0T. It can be seen that the velocity increases along the length of the pipe when the magnet field is excluded.

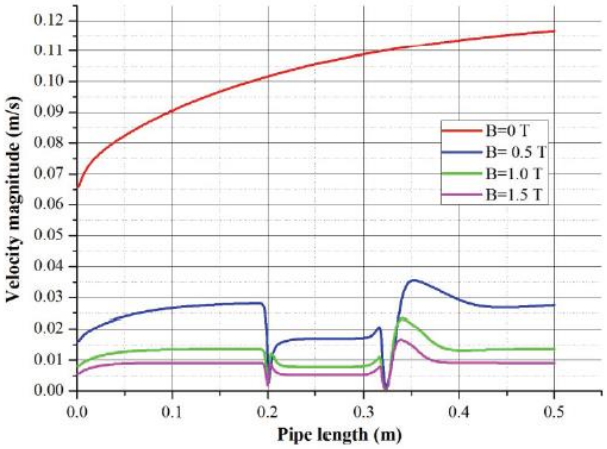

Figure 3.Velocity distributions along the length of the pipe, Gedik *et al* [8]

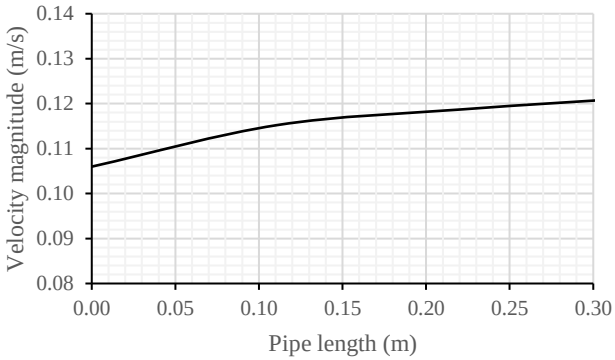

Figure 4. Velocity distributions along the length of the pipe at B = 0T, the current study

III. RESULTS AND DISCUSSION

A. *Velocity distribution*

Figure 5 shows how the velocity magnitude increases in the region of the magnet. It from 0 m/s as an initial value, although the inlet velocity was set at 0.1 m/s. Its velocity profile depicts a laminar type (the region of the magnet) and a turbulent type after the magnet towards the outlet. The proximity of the electrode to the outlet attracts the *x*-component of the velocity from its electrical potential.

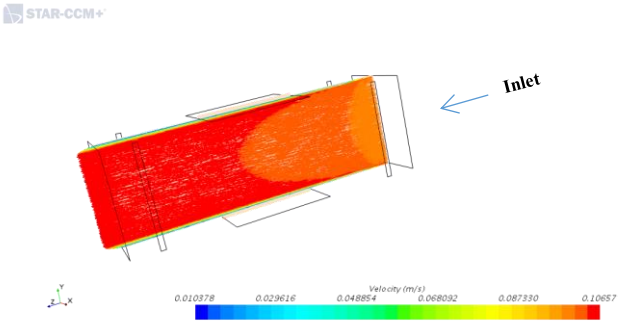

Figure 5. Velocity vector for 5V potential at 1.12T

This makes the velocity of the MHD to increase [7]. The electric field further shapes the boundary layer of the MHD by the walls to proving that the applied magnetic field is manifested as thermal energy at the boundary layer [9]. This phenomenon shows that in the absence of slip, the governing equations collapse onto the no-slip study considered [10].

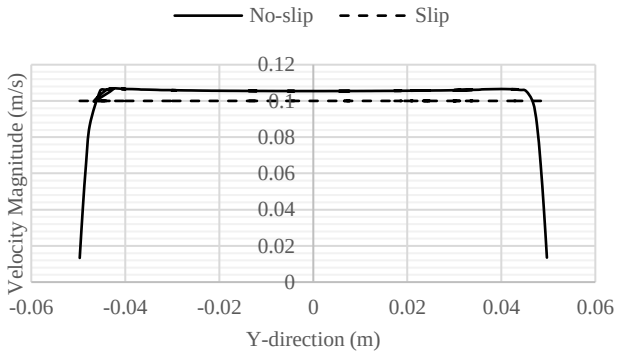

Figure 6. No-slip and slip velocity magnitude of 5V at the outlet

B. *Magnetic and Electric fields*

The isosurface of seen in Figure 7 indicates a distribution of the magnetic field. It can be deduced that along the *z*-direction (negative direction) the flow will experience its transverse pullback towards the inlet. This is because the magnetic field generates the Lorentz force that opposes the flow [5] [11]. Therefore, its strength can be a determining factor in the breakup of the boundary layer of the MHD fluid and how much on it can decelerate the flow [12].

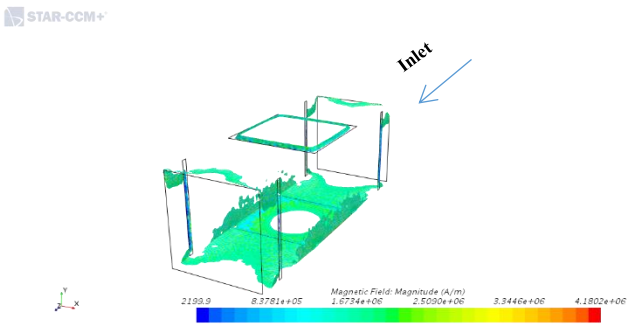

Figure 7. Isosurface of the magnetic field around the aluminum casting for 5V potential at B = 1.12T

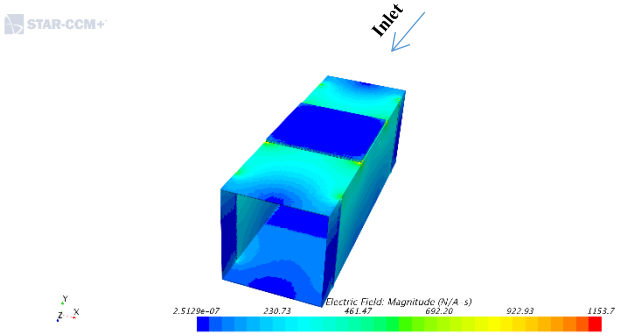

Figure 8. The electric field generated from a B = 1.12T magnet and electrodes with 5V potential

The electrical field is shown in Figure 8. Factually, the electrical potential across the electrodes will lead to an intensified current density [7] [13]. This result in increased velocity magnitude of the MHD fluid. It can be used to increase or decrease the force exerted on the fluid [14]. In that way, there can be a manipulation of the fluid flow by a careful arrangement of magnets [15].

IV. CONCLUSION

The electric field is perpendicular to both the magnetic field and the direction of the longitudinal velocity in the boundary layer. It is responsible for increasing the slip because it reduces the shear stresses between the surface of the fluid [3]. Galinstan as a dilatant fluid exhibits the same velocity decrease due to the Lorentz force and it stretches the boundary layer. The inertial effects appear to be more relevant and can enable the computation of the slip length due to an induced magnetic field.

The magnetic field **B(x)** in the x-direction being perpendicular to the laminar boundary layer pulls the fluid. It also means that the increase in the magnetic field causes the velocity to decrease. This can be seen as a means of controlling the velocity of the fluid.

The authors will be in the future investigate the secondary-velocity of MHD under the influence magnetic field on the below-mentioned fields of studies. The study will still be a numerical approach to find:

a) The effects of varying Hartmann number as an influence of Lorentz force that opposes the flow [16].

b) Lorentz force on the MHD fluid in the boundary layer on how the boundary layer separation can be controlled using the magnetic field [17].

ACKNOWLEDGMENT

The authors would like to thank the University of Johannesburg for the financial support and software used in this study.

V. BIBLIOGRAPHY

[1] S. Chaudhary and M. K. Choudhary, "Finite element analysis of magnetohydrodynamic flow over flat surface moving in parallel free stream with viscous dissipation and Joule heating," *Engineering Computations*, vol. 35, no. 4, pp. 1675-1693, 2017.

[2] J. J. Shu, J. B. Melvin and W. K. Chan, "Fluid Velocity Slip and Temperature Jump at a Solid Surface," *Applied Mechanics Reviews*, vol. 69, no. 2, pp. 1-32, 2017.

[3] M. Turkyilmazoglu, "Dual and triple solutions for MHD slip flow of non-Newtonian fluid over a shrinking surface," *Computers & Fluids*, vol. 70, pp. 53-58, 2012.

[4] A. R. Krishnan and B. S. Jinshah, "Magnetohydrodynamic power generation," *International Journal of Scientific and Research Publications*, vol. 3, no. 6, pp. 2250-3153, 2013.

[5] M. B. Ashraf, T. Hayat, S. A. Shehzad and B. Ahmed, "Thermophoresis and MHD mixed convection three-dimensional flow of viscoelastic fluid with Soret and Dufor effects," *Neural Comput & Appl*, vol. 31, pp. 249-261, 2019.

[6] Y. Wang and L. Zhang, "Fluid flow-related transport phenomena in steel slab continuous casting strands under electromagnetic brake," *Metallurgical and Materials Transactions B*, vol. 42B, pp. 2011-1319, 2011.

[7] A. O. Ayeleso, M. T. Kahn and A. K. Raji, "Computational Fluid Domain simulation of MHD flow of an ionised gas inside a rectangular duct," in *13th International Conference on the Industrial and Commercial Use of Energy*, Cape Town, South Africa, 2016.

[8] E. Gedik, H. Kurt and Z. Recebli, "CFD Simulation of Magnetohydrodynamic Flow of a liquid metal Galinstan fluid in circular pipes," *FDMP*, vol. 9, no. 1, pp. 22-33, 2013.

[9] M. S. Alam, M. R. Islam, M. R. Ali, M. A. Alim and M. M. Alam, "Magnetohydrodynamic Boundary Layer Flow of Non-Newtonian Fluid and Combined Heat and Mass Transfer about an inclined stretching sheet," *Open Journal of Applied Sciences*, vol. 5, pp. 729-294, 2015.

[10] M. Dimian, "Effect of the magnetic field on forced convection flow along a wedge with variable viscosity," *Mechanics and Mechanical Engineering*, vol. 7, no. 1, pp. 107-120, 2004.

[11] K. Jin, S. P. Vanka, B. G. Thomas and X. Ruan, "Large Eddy Simulations of the effects of double-ruler electromagnetic braking and nozzle submergence depth on molten steel flow in a commercial continuous casting mold," *CFD Modeling and Simulation in Materials Processing*, pp. 1-8, 2016.

[12] P. K. Rout, S. N. Sahoo, G. C. Dash and S. R. Mishra, "Chemical reaction effect on MHD free convection flow in a micropolar fluid," *Alexandria Engineering Journal*, vol. 6, no. 55, pp. 2967-2973, 2016.

[13] C. Vives and R. Ricou, "Experimental Study of continuous electromagnetic casting of Aluminum alloys," *Metallurgical Transactions B*, vol. 16B, pp. 377-384, 1985.

[14] M. M. Ali, M. A. Alim and L. S. Andallah, "Conjugate Effects of Radiation and Joule Heating on Magnetohydrodynamic Free Convection Flow along a Sphere with Heat Generation," *American Journal of Computational Mathematics*, vol. 1, pp. 18-25, 2011.

[15] S. M. Cho, B. G. Thomas and S. H. Kim, "Transient two-phase flow in slide-gate nozzle and mold of continous steel slab casting with and without double-ruler electro-magnetic braking".

[16] T. Hayat, S. A. Shehzad and A. Alsaedi, "Soret and Dufour effects on magnetohydrodynamic (MHD) flow of Casson fluid," *Appl. Math. Mech-Engl*, vol. 33, no. 10, pp. 1301-1312, 2012.

[17] D. Pal and S. Biswas, "Influence of Chemical Reaction and Soret Effect on Mixed Convective MHD Oscillatory Flow of Casson fluid with thermal radiation and viscous dissipation," *Int. J. Appl. Comput. Match*, vol. 3, pp. 1897-1919, 2017.

VI. NOMENCLATURE

A	Slip parameter, (-)
D	Hydraulic diameter, (m)
B	Magnetic flux density vector, (T)

$\mathbf{B_0}$	Applied magnetic field, (T)
$\boldsymbol{b}$	Induced magnetic field induction vector, (T)
$\mathbf{E}$	Applied external electrical field intensity vector, (V/m)
$\boldsymbol{Ha}$	Hartmann number
$\mathbf{J}$	Electrical current density vector, (A/m^2)
$\boldsymbol{L}$	Characteristic length of the MHD, (m)
$\boldsymbol{n}$	Casson parameter, (-)
$\mathbf{P}$	Pressure gradient, (Pa)
$\mathbf{V}$	Velocity vector, (m/s)
$\boldsymbol{x,y,z}$	Coordinate

Greek letters

η	Dynamic viscosity, (kg/ms)
ρ	Density, (kg/m^3)
σ	Electrical conductivity, (1/Ωm)
μ_e	Magnetic permeability, (H/m)